This article has been accepted for publication in a future issue of this journal, but has not been fully edited. Content may change prior to final publication. Citation information: DOI 10.1109/LWC.2016.2631602, IEEE Wireless Communications Letters

Zero-Forcing Precoding Performance in Multiuser MIMO Systems With Heterogeneous Ricean Fading

Harsh Tataria, *Student Member, IEEE*, Peter J. Smith, *Fellow, IEEE*,
Larry J. Greenstein, *Life Fellow, IEEE*, and Pawel A. Dmochowski, *Senior Member, IEEE*

***Abstract*—An accurate approximation is developed for the distribution of the instantaneous per-terminal signal-to-noise-ratio (SNR) of a downlink multiuser multiple-input multiple-output system with zero-forcing (ZF) precoding. Our analysis assumes a Ricean fading environment, where we show that the SNR at a given terminal is well approximated by the gamma distribution and derive its parameters. The analysis relies on densities of an arbitrary and a pair of arbitrary eigenvalues of uncorrelated complex non-central Wishart matrices. Unlike previous studies, we consider microwave and millimeter-wave channel parameters with a unique Rice factor for each terminal. We demonstrate that stronger line-of-sight adversely impacts the ZF SNR, whilst increasing the Rice factor variability results in higher peak ZF SNR. Our approximations are insensitive to changes in the system dimension and operating SNRs.**

***Index Terms*—Gamma distribution, SNR, ZF precoding, multiuser MIMO.**

I. Introduction

DUE to the broadcast nature of the downlink channel, multiuser multiple-input multiple-output (MU-MIMO) systems are known to suffer from inter-user interference [1]. This leads to a lower signal-to-interference-plus-noise-ratio (SINR) and spectral efficiency at the user terminal, motivating the use of spatial pre-processing techniques at the base station (BS) [2]. With channel knowledge at the BS, linear methods such as zero-forcing (ZF) precoding have been identified as more practical due to their lower complexity in comparison with the optimal, non-linear dirty-paper coding [1, 2].

Numerous works have theoretically characterized the SINR and spectral efficiency gains of downlink MU-MIMO systems with linear processing (see [1, 2] and references therein). However, the majority of these works employ the simple Rayleigh fading model which does not capture the presence of line-of-sight (LoS), anticipated to be a dominant feature in the forthcoming small cellular systems [3]. As a result, understanding the performance of MU-MIMO systems with LoS is of increasing relevance and importance. Relatively few works have considered Ricean fading in the above context, see [4–6], where the focus has largely been on characterizing the ergodic sum-rate and energy efficiency performance, rather than per-terminal performance. For simplicity, [4, 5] evaluate the system performance with a fixed Rice (K) factor for each terminal, despite variations around their local terrain.

In contrast to [4–6], we examine the effects of LoS on the instantaneous per-terminal signal-to-noise-ratio (SNR) of a downlink MU-MIMO system with ZF precoding. Considering both microwave and mmWave channel parameters, we derive an approximation to the distribution of the ZF SNR. We show that it is well approximated by the gamma distribution and derive the necessary parameters. Our approximation is accurate over a wide range of operating SNRs, system dimensions, LoS strength and LoS heterogeneity. To the best of the authors' knowledge, this level of accuracy over such a wide range of scenarios has not been achieved previously. Whilst the ZF performance reduces with an increasing specular component to the channel, we demonstrate that with a fixed mean, increasing the variability of the Rice factors leads to an increase in the peak ZF SNR due to the onset of lower Rice factor values.

Notation: Boldface upper and lower case symbols represent matrices and vectors. Transpose, Hermitian transpose, inverse and trace operators are denoted by $(\cdot)^{\mathrm{T}}$, $(\cdot)^{\mathrm{H}}$, $(\cdot)^{-1}$ and $\mathrm{tr}\{\cdot\}$, respectively. $\boldsymbol{h} \sim \mathcal{CN}\left(\mu, \sigma^2\right)$ denotes a complex Gaussian distribution for $\boldsymbol{h}$, where each element of $\boldsymbol{h}$ has mean μ and variance σ^2. $||\cdot||_{\mathrm{F}}$ and $|\cdot|$ denote the Frobenius and scalar norms, while $\mathrm{diag}\left(\boldsymbol{h}\right)$ denotes the diagonal matrix generated from $\boldsymbol{h}$. $\mathbb{E}\left[\cdot\right]$, $\mathrm{Var}\left[\cdot\right]$ and $\lfloor\cdot\rfloor$ represent the statistical expectation, variance and floor operators, respectively.

II. System Model

The downlink of a single-cell, MU-MIMO system in an urban microcellular (UMi) environment is considered. The BS, located at the center of a circular cell with radius R, is equipped with a uniform linear array (ULA) of M transmit antennas, simultaneously serving L single-antenna terminals $(M \geq L)$ in the same time-frequency interval.

A. Channel Model

We assume that the $1 \times M$ normalized fading channel between the BS and the l-th terminal has a Ricean distribution and is denoted by

$$\boldsymbol{h}_l = \sqrt{\frac{K_l}{K_l+1}}\bar{\boldsymbol{h}}_l + \sqrt{\frac{1}{K_l+1}}\tilde{\boldsymbol{h}}_l. \tag{1}$$

The specular (LoS) and diffuse (scattered) components of the channel are denoted by $\bar{\boldsymbol{h}}_l$ and $\tilde{\boldsymbol{h}}_l$, respectively. K_l denotes the ratio between the power of the specular and diffuse components for terminal l and is known as the Rice (K) factor. We note that K_l is unique to the l-th terminal and is dependent on the geographical terrain in its proximity.

Manuscript received September 29, 2016; accepted November 15, 2016. The associate editor coordinating the review of this paper and approving it for publication was Z. Rezki.

H. Tataria and P.A. Dmochowski are with the School of Engineering and Computer Science, Victoria University of Wellington, Wellington, New Zealand (e-mail: harsh.tataria, pawel.dmochowski@ecs.vuw.ac.nz).

P.J. Smith is with the School of Mathematics and Statistics, Victoria University of Wellington, Wellington, New Zealand (e-mail: peter.smith@vuw.ac.nz).

L.J. Greenstein is with the Wireless Information Network Laboratory (WINLAB), Rutgers University, North Brunswick, NJ, USA (e-mail: ljg@winlab.rutgers.edu).

This article has been accepted for publication in a future issue of this journal, but has not been fully edited. Content may change prior to final publication. Citation information: DOI 10.1109/LWC.2016.2631602, IEEE Wireless Communications Letters

Whilst $\tilde{\boldsymbol{h}}_l \sim \mathcal{CN}(0,1)$, the specular component of the channel is governed by the far-field ULA steering response, $\bar{\boldsymbol{h}}_l = \left[1, e^{j2\pi d\cos(\varphi_l)}, \ldots, e^{j2\pi d(M-1)\cos(\varphi_l)}\right]$. Here, d denotes the equidistant antenna spacing normalized by the carrier wavelength and φ_l is the azimuth angle-of-departure (AoD) of the specular component, for the l-th terminal. In this study, we consider uncorrelated propagation, thus we set the inter-element spacing to a half-wavelength at the BS and assume that the AoDs are uniformly distributed on $[0, 2\pi]$. From (1), the composite $L \times M$ fast-fading channel matrix can also be written as

$$\boldsymbol{H}_{\text{c}} = \sqrt{\boldsymbol{\Psi}}\left(\sqrt{K_{\text{av}}}\,\bar{\boldsymbol{H}} + \tilde{\boldsymbol{H}}\right) = \sqrt{\boldsymbol{\Psi}}\boldsymbol{H}, \tag{2}$$

where $K_{\text{av}} = (1/L)\sum_{l=1}^{L} K_l$, $\boldsymbol{\Psi} = \text{diag}\left(\frac{1}{K_1+1}, \ldots, \frac{1}{K_L+1}\right)$ is an $L \times L$ matrix, $\bar{\boldsymbol{H}} = \left[\sqrt{\frac{K_1}{K_{\text{av}}}}\bar{\boldsymbol{h}}_1^{\text{T}}, \ldots, \sqrt{\frac{K_L}{K_{\text{av}}}}\bar{\boldsymbol{h}}_L^{\text{T}}\right]^{\text{T}}$ is the $L \times M$ specular channel matrix and $\tilde{\boldsymbol{H}}$ is the $L \times M$ diffuse channel matrix containing $\mathcal{CN}(0,1)$ entries, respectively. We model the distribution of terminals with a uniform density with respect to the coverage area of the cell. An exclusion radius of r_0 is assumed, such that the closest terminal to the BS is a distance r_0 away. The received power at the l-th terminal is denoted by $\tilde{\beta}_l = \rho A \zeta_l (r_0/r_l)^{\tau}$ and is composed of the total transmit power, ρ, with large-scale fading effects. In particular, A is the unit-less constant for geometric attenuation at a reference distance r_0, r_l is the link distance between the BS and terminal l, τ is the attenuation exponent and ζ_l represents the effects of log-normal shadowing, i.e., $10\log_{10}(\zeta_l) \sim \mathcal{N}\left(0, \sigma_{\text{sh}}^2\right)$.

Since $\boldsymbol{\Psi}$ simply scales the terminal channels, the *overall* channel can be viewed as a small-scale fading channel matrix, $\boldsymbol{H}$, with equivalent received powers, $\beta_l = \boldsymbol{\Psi}_{l,l}\tilde{\beta}_l = \tilde{\beta}_l (K_l+1)^{-1}$. This *overall* channel is used throughout the paper, which allows us to leverage previous analytical results on channels of the form in (2). For the remainder of the paper, the received SNR is defined as the ratio of the long term received signal power to the noise power at the terminal.

B. ZF Precoding and Per-Terminal SNR

The received signal at terminal l can be expressed as

$$y_l = \sqrt{\frac{\beta_l}{\eta}}\boldsymbol{h}_l \boldsymbol{g}_l s_l + z_l, \tag{3}$$

where $\boldsymbol{h}_l$ is the l-th row of $\boldsymbol{H}$, $\boldsymbol{g}_l$ is the un-normalized precoding vector for terminal l, s_l is the data symbol desired for terminal l, with $\mathbb{E}\left[|s_l|^2\right] = 1$, η is the precoding normalization parameter and $z_l \sim \left(0, \sigma_l^2\right)$ is the additive white Gaussian noise at terminal l. We consider ZF precoding to design the downlink precoding vectors, where $\boldsymbol{g}_l$ is the l-th column of the $M \times L$ precoding matrix, $\boldsymbol{G} = \boldsymbol{H}^{\text{H}}\left(\boldsymbol{H}\boldsymbol{H}^{\text{H}}\right)^{-1}$. The precoding matrix is normalized by $\eta = ||\boldsymbol{G}||_{\text{F}}^2/L$, ensuring that the total transmit power remains ρ. From (3), the ZF SNR for terminal l is defined as

$$\text{SNR}_l^{\text{ZF}} = \frac{\beta_l}{\sigma_l^2\eta} = \frac{\beta_l}{\sigma_l^2\,\text{tr}\{(\boldsymbol{H}\boldsymbol{H}^{\text{H}})^{-1}\}}. \tag{4}$$

III. Distributional Approximation to the ZF Per-Terminal SNR

The distribution of the ZF SNR in (4) is particularly difficult to analyze, since it is a random function of the uncorrelated complex non-standard, non-central Wishart matrix formed by $\boldsymbol{H}\boldsymbol{H}^{\text{H}}$. Hence, analytical expressions for the probability density and cumulative distribution appear intractable. Therefore, we approximate the distribution of the ZF SNR with the gamma distribution. Our motivation for considering the gamma distribution comes from previous studies which have shown that in the case when no LoS is present (i.e., Rayleigh fading), the ZF SNR follows the chi-squared distribution [7], a special case of the gamma distribution. More general studies with minimum-mean-squared-error (MMSE) receive combining under spatially correlated Rayleigh fading [8] and the presence of LoS (where the desired terminal is subject to Ricean fading, whilst the multiuser interference is subject to Rayleigh fading [9]) have shown that the MMSE SINR is well approximated by the gamma distribution. Here, with ZF precoding, we further extend the above results considering the most general scenario where *each* terminal (desired or interfering) experiences Ricean fading with a unique Rice factor. In order to make such an approximation, the shape and scale parameters of the gamma distribution have to be derived, as shown in the subsequent theorem.

Theorem: If the channel to terminal l follows a Ricean distribution and SNR_l^{ZF} is modeled as a gamma random variable, then $\delta = \text{tr}\{\left(\boldsymbol{H}\boldsymbol{H}^{\text{H}}\right)^{-1}\}$ follows an inverse gamma distribution, denoted by $\Gamma(\alpha, \varrho)^{-1}$, with the shape and scale parameters

$$\alpha = 2 + \frac{\mathbb{E}[\delta]^2}{\text{Var}[\delta]} \text{ and } \varrho = \frac{\beta_k}{\left\{1 + \frac{\mathbb{E}[\delta]^2}{\text{Var}[\delta]}\right\}\mathbb{E}[\delta]}, \tag{5}$$

Proof: α and ϱ are derived via the method of moments. If δ^{-1} is $\Gamma(\alpha, \varrho)$, using its standard properties we observe that

$$\mathbb{E}\left[\delta^{-1}\right] = \left((\alpha-1)\varrho\right)^{-1}, \tag{6}$$

and

$$\text{Var}\left[\delta^{-1}\right] = \left((\alpha-1)(\alpha-2)\varrho^2\right)^{-1}. \tag{7}$$

Note that re-arranging (6) and (7) allows us to derive (5). Moreover, $\delta = \text{tr}\{\left(\boldsymbol{H}\boldsymbol{H}^{\text{H}}\right)^{-1}\} = \sum_{i=1}^{L}\lambda_i^{-1}$, where λ_i is the i-th eigenvalue of $\boldsymbol{H}\boldsymbol{H}^{\text{H}}$. From here it is straightforward to show that $\mathbb{E}[\delta] = L\mathbb{E}\left[\lambda^{-1}\right]$, where λ is an arbitrary eigenvalue of $\boldsymbol{H}\boldsymbol{H}^{\text{H}}$. Also, as $\text{Var}[\delta] = \mathbb{E}\left[\sum_{i=1}^{L}\sum_{j=1}^{L}(\lambda_i\lambda_j)^{-1}\right] - L^2\mathbb{E}\left[\lambda^{-1}\right]^2$, the first term of $\text{Var}[\delta]$ can be re-written as $Y = \mathbb{E}\left[\sum_{i=1}^{L}\lambda_i^{-2} + \sum_{i=1}^{L}\sum_{j=1,j\neq i}^{L}\lambda_i^{-1}\lambda_j^{-1}\right] = L\mathbb{E}\left[\lambda^{-2}\right] + L(L-1)\mathbb{E}\left[\lambda_1^{-1}\lambda_2^{-1}\right]$, where λ_1 and λ_2 are two distinct arbitrary eigenvalues of $\boldsymbol{H}\boldsymbol{H}^{\text{H}}$. Hence, $\mathbb{E}\left[\lambda^{-1}\right]$, $\mathbb{E}\left[\lambda^{-2}\right]$ and $\mathbb{E}\left[\lambda_1^{-1}\lambda_2^{-1}\right]$ govern $\mathbb{E}[\delta]$ and $\text{Var}[\delta]$, which are derived in the subsequent analysis.

A. Calculation of $\mathbb{E}\left[\lambda^{-1}\right]$

By definition

$$\mathbb{E}\left[\lambda^{-1}\right] = \int_0^{\infty}\frac{1}{\lambda}f_{\lambda}(\lambda)\,d\lambda, \tag{8}$$

where $f_{\lambda}(\lambda)$ is the arbitrary eigenvalue density given in Theorem 1 of [10], from which (8) can be expressed as

$$\mathbb{E}\left[\lambda_1^{-1}\right] = \int_0^{\infty}\lambda^{-1}\frac{e^{-\sum_{i=1}^{L}\Phi_i}}{L\left((M-L)!\right)^L}\frac{e^{-\lambda}\left(\bar{K}+1\right)}{\lambda}\sum_{j=1}^{L}\left(\left(\bar{K}+1\right)\lambda\right)^a$$

This article has been accepted for publication in a future issue of this journal, but has not been fully edited. Content may change prior to final publication. Citation information: DOI 10.1109/LWC.2016.2631602, IEEE Wireless Communications Letters

$$\sum_{\substack{i=1\\ i\neq j}}^{L}\sum_{p=0}^{\infty}\frac{\left(\left(\bar{K}+1\right)\Phi_i\lambda\right)^p\mathcal{D}\left(i,j\right)}{p!\left(M-L+1\right)_p}\Bigg/\left\{\prod_{k<q}^{L}(\Phi_q-\Phi_k)\right\}d\lambda, \quad (9)$$

where $a=M-L+j$, Φ_i is the i-th eigenvalue of $\bar{K}\bar{\boldsymbol{H}}\bar{\boldsymbol{H}}^{\mathrm{H}}$, $(a)_b=\frac{(a+b-1)!}{(a-1)!}$ and $\mathcal{D}\left(i,j\right)$ is the (i,j)-th co-factor of an $L\times L$ matrix $\boldsymbol{A}$, whose (l,k)-th entry is $(\boldsymbol{A})_{l,k}=(M-L+k-1)!\;{}_1F_1\left(M-L+k,M-L+1,\Phi_l\right)$, with ${}_1F_1$ being the Kummer confluent hypergeometric function. Extracting the constants and simplifying (9) yields

$$\mathbb{E}\left[\lambda_1^{-1}\right]=\frac{e^{-\sum_{i=1}^{L}\Phi_i}}{L\left((M-L)!\right)^L}\frac{1}{\prod_{k<q}^{L}\left(\Phi_q-\Phi_k\right)}\sum_{j=1}^{L}\sum_{i=1}^{m}\sum_{p=0}^{\infty}\left(\bar{K}+1\right)^a \frac{\left(\left(\bar{K}+1\right)\Phi_i\right)^p\mathcal{D}\left(i,j\right)}{p!\left(M-L+1\right)_p}\int_0^{\infty}\lambda^{M-L+j+p-2}e^{-\lambda\left(\bar{K}+1\right)}d\lambda. \quad (10)$$

Denoting $t=M-L+j+p-2$, the integral in (10) can be solved in closed-form as

$$\int_0^{\infty}\lambda^t e^{-\lambda\left(\bar{K}+1\right)}d\lambda=t!\left(\bar{K}+1\right)^{-t-1}. \quad (11)$$

Substituting the solution of the integral in (11) and multiplying the resultant expression by L yields an expression for $\mathbb{E}\left[\delta\right]$.

B. Calculation of $\mathbb{E}\left[\lambda^{-2}\right]$

Following the methodology in the calculation of $\mathbb{E}\left[\lambda^{-1}\right]$, $\mathbb{E}\left[\lambda^{-2}\right]$ has the exact same form as $\mathbb{E}\left[\lambda^{-1}\right]$, where t in (10) and (11) is replaced by $\tilde{t}=M-L+j+p-3$.

C. Calculation of $\mathbb{E}\left[\lambda_1^{-1}\lambda_2^{-1}\right]$

In order to evaluate Y, the first term of $\mathrm{Var}\left[\delta\right]$, we require $\mathbb{E}\left[\lambda_1^{-1}\lambda_2^{-1}\right]$. By definition

$$\mathbb{E}\left[\lambda_1^{-1}\lambda_2^{-1}\right]=\int_0^{\infty}\int_0^{\infty}\lambda_1^{-1}\lambda_2^{-1}f_{\lambda_1,\lambda_2}\left(\lambda_1,\lambda_2\right)d\lambda_1 d\lambda_2, \quad (12)$$

where $f_{\lambda_1,\lambda_2}\left(\lambda_1,\lambda_2\right)$ is the recently derived joint density of two distinct arbitrary eigenvalues, (λ_1,λ_2), as presented in Theorem 2 of [6]. Thus, (12) can be written as

$$\mathbb{E}\left[\lambda_1^{-1}\lambda_2^{-1}\right]=\int_0^{\infty}\int_0^{\infty}\Theta\sum_{i=0}^{L-1}\sum_{j=0}^{L-1}\sum_{u=1}^{L}\sum_{v=1}^{L}\left(-1\right)^w\tilde{\boldsymbol{\Xi}}\left(u,v;i,j\right) X_{u,i}\left(\lambda_1\right)X_{v,j}\left(\lambda_2\right)d\lambda_1\,d\lambda_2, \quad (13)$$

where $\Theta=\chi\left\{(\omega-1)!\right\}^L\left(-1\right)^{\lfloor\frac{L}{2}\rfloor}(M-2)!$ with $\chi=\frac{e^{-\sum_{i=1}^{L}\Phi_i}}{L((M-L)!)^L\prod_{k<q}^{L}(\Phi_q-\Phi_k)}$ and $\omega=M-L+1$, respectively. Moreover, $w=i+j+u+v-p\left(i,j\right)-x\left(u,v\right)$ with

$$p(i,j)=\begin{cases}0\;;j\leq i\\1\;;j>i\end{cases}\text{ and }x(u,v)=\begin{cases}0\;;v\leq u\\1\;;v>u,\end{cases} \quad (14)$$

while $\tilde{\boldsymbol{\Xi}}\left(u,v;i,j\right)=\left(\Phi_u\Phi_v\right)^{-(M-L)/2}\boldsymbol{\Xi}\left(u,v;i,j\right)$ where $\boldsymbol{\Xi}\left(u,v;i,j\right)$ is a $L\times L$ determinant with rows u,v and columns i,j removed, with the d-th entry in the f-th column is given by $\Gamma\left(\omega+f-1\right)/\Gamma\left(M-L+1\right)_1F_1(M-L+f,M-L+1,\Phi_d)$. Here, $\Gamma\left(\cdot\right)$ denotes the gamma function. $X_{a,b}\left(\lambda\right)=\lambda^{(M-L)/2+b}\,e^{-\lambda}\mathrm{I}_{M-L}\left(2\sqrt{\Phi_a\lambda}\right)$, where $\mathrm{I}_{M-L}\left(\cdot\right)$ is a modified Bessel function of the first kind. Substituting the definition of $X_{u,i}\left(\lambda_1\right)$ and $X_{v,j}\left(\lambda_2\right)$ into (13) and performing some mathematical simplifications results in

$$\mathbb{E}\left[\lambda^{-1}\lambda_2^{-1}\right]=\Theta\sum_{i=0}^{L-1}\sum_{j=0}^{L-1}\sum_{u=1}^{L}\sum_{v=1}^{L}\left(-1\right)^w\tilde{\boldsymbol{\Xi}}\left(u,v;i,j\right)\Delta_{u,i}\left(\lambda_1\right)\Delta_{v,j}\left(\lambda_2\right), \quad (15)$$

where $\Delta_{a,b}\left(\lambda\right)=\int_0^{\infty}\lambda^{((M-L)/2)+b-1}e^{-\lambda}\mathrm{I}_{M-L}\left(2\sqrt{\Phi_a\lambda}\right)d\lambda$. For $M-L\geq 1$ and $b>0$, the above integral is given in closed form in [11, Eq. (6.643.2)]. For $M-L=0$ and $b=0$, a series expansion solution is required, as in [6]. Thus, the first term of $\mathrm{Var}\left[\delta\right]$, Y, can be expressed as (16). Subtracting $L^2\mathbb{E}\left[\lambda^{-1}\right]^2$ from (16) yields the expression for $\mathrm{Var}\left[\delta\right]$, concluding the proof. ■

D. Remarks

(i) In the derivation of $\mathbb{E}\left[\delta\right]$ and $\mathrm{Var}\left[\delta\right]$, we used the eigenvalue densities, $f_{\lambda}\left(\lambda\right)$ and $f_{\lambda_1,\lambda_2}\left(\lambda_1,\lambda_2\right)$, of the instantaneous channel correlation matrix, $\boldsymbol{H}\boldsymbol{H}^{\mathrm{H}}$, which has an uncorrelated complex non-central Wishart structure. This is in contrast to other work where a further approximation was made [4, 5] by approximating the non-central structure by its central equivalent via an adjustment of the covariance matrix.

(ii) The result holds for any system dimension (number of serving antennas at the BS and terminals in the system) and operating SNR. Moreover, the result is robust to the level of LoS present in the system. It also remains tight for Rayleigh fading channels which exhibit no LoS effects. Our analysis methodology can easily be extended to other system types, such as multicellular systems and distributed antenna arrays due to the general structure of the ZF SNR in (4).

IV. Numerical Results

We employ a statistical approach to determine whether a given terminal experiences LoS or non-LoS (NLoS) propagation. The NLoS and LoS probabilities are governed by the link distance, from which other link characteristics such as the attenuation exponent and shadow-fading standard deviation are selected. We consider UMi propagation parameters for microwave [12] and mmWave [13, 14] frequencies at 2 and 28 GHz, respectively. For both cases, the cell radius (R), the exclusion area (r_0) and the transmit power (ρ) are fixed to 100 m, 10 m and 30 dBm, respectively. Noise variances of -120 dBm and -113 dBm are obtained at 20 and 100 MHz bandwidths for the microwave and mmWave cases, whilst the LoS and NLoS attenuation exponents (τ) are given by 2.2, 3.67 and 2, 2.92 at microwave and mmWave, respectively. The LoS attenuation constants (A) are 28 dB and 61.4 dB, whilst the NLoS attenuation constants are 22.7 and 72 dB. Moreover, LoS and NLoS shadow-fading standard deviations (σ_{sh}) are 3, 4 and 5.8, 8.7 for the microwave and mmWave cases. The Ricean K-factor has a log-normal density with a mean of 9 and standard deviation of 5 dB for microwave ($K\sim\ln\left(9,5\right)$) [12] and a mean of 12 and standard deviation of 3 dB for the mmWave ($K\sim\ln\left(12,3\right)$) [14] cases, respectively. At microwave, the probability of terminal l experiencing LoS is given by $P_{\mathrm{LoS}}\left(r_l\right)=\left(\min\left(18/r_l,1\right)\left(1-e^{-r_l/36}\right)\right)+e^{-r_l/36}$. Equivalently, at mmWave $P_{\mathrm{LoS}}=\left(1-P_{\mathrm{out}(r_l)}\right)e^{-\iota_{\mathrm{LoS}}r_l}$, where $1/\iota_{\mathrm{LoS}}=67.1$ meters and P_{out}, the outage probability is set to 0 for simplicity. Naturally, for both cases, $P_{\mathrm{NLoS}}=1-P_{\mathrm{LoS}}$.

With $M=30$ and $L=3$, Fig. 1 demonstrates the accuracy of the derived approximation in response to changes in the operating SNRs. In addition to the microwave and mmWave

This article has been accepted for publication in a future issue of this journal, but has not been fully edited. Content may change prior to final publication. Citation information: DOI 10.1109/LWC.2016.2631602, IEEE Wireless Communications Letters

$$Y = \left[L \left\{ \chi \sum_{j=1}^{L} \sum_{i=1}^{L} \sum_{p=0}^{\infty} \left(\bar{K}+1\right)^{a} \frac{\left(\left(\bar{K}+1\right)\Phi_i\right)^{p} \mathcal{D}\left(i,j\right)}{p!\left(M-L+1\right)_p} \tilde{t}!\left(\bar{K}+1\right)^{-\tilde{t}-1} \right\} + L\left(L-1\right) \left\{ \mathbb{E}\left[\left(\lambda_1\lambda_2\right)^{-1}\right] \right\} \right]. \quad (16)$$

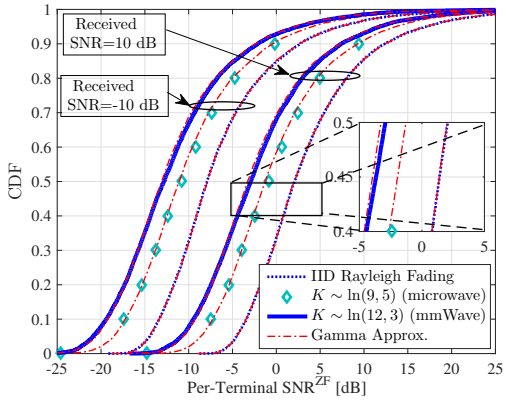

Fig. 1. Per-Terminal SNR^{ZF} with $M = 30$, $L = 3$ at received SNR=-10 dB and 10 dB.

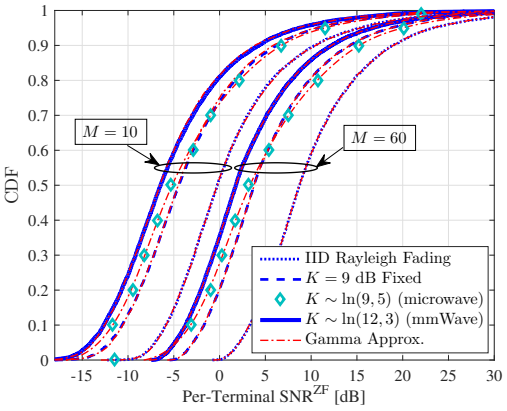

Fig. 2. Per-Terminal SNR^{ZF} at received SNR $= 10$ dB with $L = 3$, $M = 10$ and 60.

cases, we consider the case when no LoS is present, i.e., Rayleigh fading, as a baseline for comparison. Two trends can be observed: (1) Increasing the mean of K adversely affects the terminal SNR. This is due to the fact that with a fixed transmit power, an increase in the mean of K implies a stronger specular component in the channel, which reduces the amount of multi-path and in-turn results in a lower channel rank. Equivalently, this effect can be interpreted as an increase in the level of channel correlation leading to fewer usable spatial degrees of freedom; (2) The proposed approximations are insensitive to changes in SNRs and only the most marginal deviation between the simulated and approximated responses can be observed for both microwave and mmWave cases. The approximations also remain tight in the Rayleigh fading case, consistent with Remark (ii). In Fig. 2, we evaluate the accuracy of the proposed approximation with increasing numbers of BS antennas at SNR=10 dB with $L = 3$. Naturally, increasing the number of serving antennas leads to higher terminal SNRs. We also study the effects of Rice factor heterogeneity, where we show that increasing the variability of the Rice factor from $K = 9$ dB fixed for all terminals to a variable K with a mean of 9 dB enhances the peak ZF SNR. This is because a wider log-normal density allows for very low Rice factors to be drawn, resulting in improved performance. In contrast to this, the cell-edge and median ZF SNRs tend to reduce, as the magnified Rice factor variability also produces large Rice factors. In addition to the above, we can readily observe that our approximations retain their tightness and are robust to changes in the system size, consistent with Remark (ii).

V. Conclusion

We have presented an approximation to the distribution of the instantaneous per-terminal SNR of a ZF MU-MIMO system. We show that the ZF SNR approximately follows a gamma distribution and derive its parameters. The approximation is robust to changes in system size, SNRs and can be applied to both LoS and NLoS channels. Densities of an arbitrary and a joint pair of arbitrary eigenvalues were instrumental in deriving the gamma parameters. With microwave and mmWave parameters, our results indicate that increasing the specular component of the channel reduces the ZF SNR, whilst increasing the Rice factor variability increases the peak ZF SNR and reduces the cell-edge and median ZF SNRs.

References

[1] F. Rusek, D. Persson, B. Lau, E. Larsson, T. Marzetta, O. Edfors, and F. Tufvesson, "Scaling up MIMO: Opportunities and challenges with very large arrays," *IEEE Signal Process. Mag.*, vol. 30, no. 1, pp. 40–60, Jan. 2013.

[2] H. Yang and T. Marzetta, "Performance of conjugate and zero-forcing beamforming in large-scale antenna systems," *IEEE Journal on Sel. Topics in Commun.*, vol. 31, no. 2, pp. 172–179, Feb. 2013.

[3] S. Sun, T. Rappaport, R. Heath, A. Nix, and S. Rangan, "MIMO for millimeter-wave wireless communications: Beamforming, spatial multiplexing, or both?" *IEEE Commun. Mag.*, vol. 52, no. 12, pp. 110–121, Dec. 2014.

[4] C. Kong, C. Zhong, M. Matthaiou, and Z. Zhang, "Performance of downlink massive MIMO in Ricean fading channels with ZF precoder," in *Proc. IEEE Int. Conf. on Commun. (ICC)*, Jun. 2015, pp. 1776–1782.

[5] Q. Zhang, J. Shi, K.-K. Wong, H. Zhu, and M. Matthaiou, "Power scaling of uplink massive MIMO systems with arbitrary-rank channel means," *IEEE J. Sel. Topics Signal Process.*, vol. 8, no. 5, pp. 966–981, Oct. 2014.

[6] H. Tataria, P. Smith, L. Greenstein, P. Dmochowski, and M. Shafi, "Performance and analysis of downlink multiuser MIMO systems with regularized zero-forcing precoding in Ricean fading channels," *in Proc. of IEEE Int. Conf. on Commun. (ICC)*, pp. 1185–1191, May 2016.

[7] D. Gore, R. Heath, and A. Paulraj, "Transmit selection in spatial multiplexing systems," *IEEE Commun. Lett.*, vol. 6, no. 11, pp. 491–493, Nov. 2002.

[8] P. Li, D. Paul, R. Narasimhan, and J. Cioffi, "On the distribution of SINR for the MMSE MIMO receiver and performance analysis," *IEEE Tras. Info. Theory*, vol. 52, no. 1, pp. 271–286, Jan. 2006.

[9] R. Louie, M. McKay, and I. Collings, "New peformance results for multiuser optimum combining in the presence of Rician fading," *IEEE Tras. Commun.*, vol. 8, no. 57, pp. 2348–2358, Aug. 2009.

[10] G. Alfano, A. Lozano, A. Tulino, and S. Verdú, "Mutual information and eigenvalue distribution of MIMO Ricean channels," in *Proc. IEEE Int. Symp. Information Theory & Applications (ISITA)*, Oct. 2004.

[11] I. Gradshteyn and I. Ryzhik, *Table of Integrals, Series, and Products*. Academic Press, 2007.

[12] 3GPP TR 36.873 v.12.2.0, *Study on 3D channel models for LTE*. 3GPP, Jun. 2015.

[13] M. Akdeniz, Y. Liu, M. Samimi, S. Sun, S. Rangan, T. Rappaport, and E. Erkip, "Millimeter wave channel modeling and cellular capacity evaluation," *IEEE J. Sel. Areas Commun.*, vol. 32, no. 6, pp. 1164–1179, Jun. 2014.

[14] T. Thomas, H. Nugyen, G. MacCartney, and T. Rappaport, "3D mmWave channel model proposal," in *Proc. IEEE Conf. on Veh. Technol. (VTC-Fall)*, Sep. 2014, pp. 1–6.